J Herbmed Pharmacol. 2024; 13(3): 491-500.

http://www.herbmedpharmacol.com doi: 10.34172/jhp.2024.52533

Journal of Herbmed Pharmacology

The cytotoxic and apoptotic activity of *Costus speciosus* (Koenig) Smith (Costaceae) leaves against MCF-7 and HeLa cells

Eli Halimah[1], Gofarana Wilar[1], Ferry Ferdiansyah Sofian[2], Sandra Megantara[3], Jutti Levita[1*]

[1]Department of Pharmacology and Clinical Pharmacy, Faculty of Pharmacy, Padjadjaran University, Sumedang-45363, West Java, Indonesia
[2]Department of Biology Pharmacy, Faculty of Pharmacy, Padjadjaran University, Sumedang-45363, West Java, Indonesia
[3]Department of Analysis Pharmacy and Medicinal Chemistry, Faculty of Pharmacy, Padjadjaran University, Sumedang-45363, West Java, Indonesia

ARTICLE INFO

Article Type:
Original Article

Article History:
Received: 4 March 2024
Accepted: 3 May 2024

Keywords:
Anticancer activity
Apoptosis
Antiproliferative activity
Cheilocostus speciosus
Cytotoxicity
Drug discovery

ABSTRACT

Introduction: *Costus cuspidatus* and *Costus subsessilis* have shown cytotoxic effects in HL60, Jurkat, and THP-1 cells. This study aimed to evaluate the cytotoxicity and apoptotic activity of the ethanol extract and fractions of *C. speciosus* leaves against MCF-7 and HeLa cells and to study the binding affinity of known phytoconstituents in *C. speciosus* toward caspase-3.
Methods: The leaves were extracted with 96% ethanol for 72 hours. The extract was further subjected to a liquid-liquid fractionation by employing water, n-hexane, and ethyl acetate solvents. The cytotoxicity of the ethanol extract (CSEE), as well as water (CSWF), n-hexane (CSHF), and ethyl acetate (CSEF) fractions on MCF-7 and HeLa cells was carried out using the CCK-8/WST-8 reagent, followed by flow cytometry analysis to obtain the apoptotic activity on both cells.
Results: On MCF-7 cells, the best cytotoxicity was exhibited by CSEF (IC50 of 58.71 µg/mL), followed respectively by CSHF, CSWF, and CSEE. On HeLa cells, the extract and fractions weakly inhibited the survival growth rate, with the best cytotoxicity respectively shown by CSEF (IC50 of 233.881 µg/mL), CSEE, and CSHF. Furthermore, the exposure of CSEF to MCF-7 cells resulted in an average of 22.9% undergoing early-stage apoptosis, to HeLa cells resulted in an average of 40.85% undergoing necrosis. Molecular docking simulation revealed that diosgenin and beta-sitosterol interacted with caspase-3 residues with considerable affinity.
Conclusion: The CSEF of *C. speciosus* leaves induces cytotoxicity, whose mechanism seems to be either at the early apoptosis stage on MCF-7 cells or by necrosis on HeLa cells.

Implication for health policy/practice/research/medical education:
This study may support the development of *Costus speciosus* (Koenig) Smith leaves as an anticancer adjuvant therapy.
Please cite this paper as: Halimah E, Wilar G, Sofyan FF, Megantara M, Levita J. The cytotoxic and apoptotic activity of *Costus speciosus* (Koenig) Smith (Costaceae) leaves against MCF-7 and HeLa cells. J Herbmed Pharmacol. 2024;13(3):491-500. doi: 10.34172/jhp.2024.52533.

Introduction

Over 35 million new cancer cases are predicted in 2050, a 77% increase from the estimated 20 million cases in 2022. Of the data obtained from 185 countries in 2022, female breast carcinoma ranked second, which was 2.3 million cases or 11.6% (1). Cancer metastasis occurs when the primary tumor cells damage and proliferate to other sites of the body (2). It is described that oxidative stress may be involved directly in the onset and development of cancer. During the neoplasia initiation stage, free radicals play a paramount role in altering the genetic material of the cells responsible for mutagenesis and carcinogenesis (3). Cisplatin is a platinum-based anticancer agent that works by alkylating deoxyribonucleic acid (DNA) and building platinum-DNA adducts, leading to DNA damage, gap1/synthesis phase (G1/S) arrest, and apoptosis. Thus, it is efficacious in eliminating cancer cells. However, in long-term use, resistance may develop (4). Therefore, discovering novel anticancer agents, particularly of natural products, may be challenging.

The numerous biological activities of medicinal plants are thought to originate from the secondary metabolite

***Corresponding author**: Jutti Levita,
Email: jutti.levita@unpad.ac.id

contents. Plants containing bioactive compounds with heterocyclic structures have been reported for their anticancer activities (5-7). In the nonpolar and semipolar fractions of the methanol extract of *Costus* genus plants, flavonoids and terpenoids were reported to be present, while saponins were found in the water-soluble fractions (8). Triterpenes have been isolated from *Costus speciosus* (Koenig) Smith, synonym *Cheilocostus speciosus* (J. Koenig) C. Specht roots. Flavonol glycosides and flavonoids were isolated from the leaves of *C. speciosus* (9). Bioactive compounds namely diosgenin, dioscin, curcumin, beta-sitosterol, stigmasterol, campestral, and many more, were identified in different parts of *C. speciosus* (10).

Interestingly, plants of the *Costus* genus have shown cytotoxic activity against numerous cancer cells. The methanol extracts of *C. speciosus* have been delineated to inhibit the growth of liver cancer cells (hepatoblastoma HepG2) (11,12), triple-negative breast cancer MD Anderson-metastasis breast cancer (MDA-MB-231) cells (8), and human colon adenocarcinoma (COLO 320DM) cells (13). The nonpolar fraction of the methanol extract could induce apoptosis via DNA damage, downregulate mutant p53, and over-express the cell cycle inhibitors p21 and p27 (8). Moreover, the crude ethanol extracts of *C. cuspidatus* and *C. subsessili*s showed cytotoxic effects in human leukemia (HL60), human T lymphocytes (Jurkat), and human acute monocytic leukemia (THP-1) cells (14). However, only limited molecular docking simulations of bioactive compounds of Costus genus plants were reported, e.g., towards cyclooxygenase (COX) enzymes for anti-inflammatory (15) and caspases for anticancer (16). Considering this, our study aimed to evaluate the cytotoxicity and apoptotic activities of the ethanol extract and fractions of *C. speciosus* leaves against human breast cancer Michigan Cancer Foundation-7 (MCF-7) and cervical cancer (HeLa) cells through *in vitro* and molecular docking studies.

Materials and Methods

Plant

The fresh leaves were collected from the Ciparay Bandung area (Google map -7.032557062301384, 107.70138324126452), West Java, Indonesia, and the plant specimen was taxonomically identified and confirmed as *Costus speciosus* (Koenig) Smith, synonym *Cheilocostus speciosus* (J. Koenig) C. Specht (herbarium No. 36/HB/2021 at the Laboratory of Plant Taxonomy, the Department of Biology, Faculty of Mathematics and Natural Sciences, Padjadjaran University, Indonesia) with descriptions as listed in https://powo.science.kew.org/taxon/urn:lsid:ipni.org:names:796383-1

Chemicals

The chemicals used were technical grade ethanol 96% (Bratachem, Bandung, Indonesia) for plant extraction, technical grade n-hexane (Alfa Omega Kimia, Tangerang, Indonesia) and technical grade ethyl acetate (Alfa Omega Kimia, Tangerang, Indonesia) for fractionation, dimethyl sulfoxide (DMSO) (Sigma-Aldrich, USA), penicillin/streptomycin (Merck, USA), cell counting kit-8 (CCK-8)/water-soluble tetrazolium salt-8 (WST-8) (Dojindo, Japan) for cytotoxicity assay, RPMI-1640 medium, human breast cancer cell lines (MCF-7 from European Collection of Authenticated Cell Cultures-ECACC) (Sigma-Aldrich, USA), human cervical cancer cell lines (HeLa from American Type Culture Collection-ATCC) (Sigma-Aldrich, USA), and fetal bovine serum (FBS) (Invitrogen, USA).

Extract preparation

Each of the fresh leaves was cleaned from the soil, dust, and other foreign inorganic matters, washed under tap water, and sun-dried for 4-5 days 6-8 hours per day. The dried leaves (770 g) were soaked in a technical grade ethanol 96% (with a ratio of 1:10) for 72 h at 25 ± 2 °C. Ethanol was chosen particularly because of its property to dissolve most all secondary metabolites and safety (17,18). The extract was collected and filtered using Whatman paper and the solvent was evaporated in a vacuum rotavapor at 50 ± 2 °C to a thick consistency. The thick ethanol extract (CSEE) was further partitioned using a mixture of water and n-hexane in a separatory funnel. The n-hexane phase (CSHF) was collected and added with ethyl acetate to obtain the ethyl acetate fraction (CSEF). Ethyl acetate is a commonly used solvent to extract polyphenols with successful yield due to its semipolar property (19).

Cell culture

The MCF-7 (European Collection of Authenticated Cell Cultures-ECACC) and HeLa (American Type Culture Collection ATCC) cell lines were the collections of the Cell and Molecular Biology Laboratory, Faculty of Pharmacy, Padjadjaran University, Indonesia. The cells were grown at 37 °C with 5% carbon dioxide (CO_2) in Roswell Park Memorial Institute (RPMI)-1640 medium supplemented with penicillin-streptomycin 100 U/mL and FBS 10% to a confluency of 80%.

Effect of *Costus speciosus* on the % survival rate of MCF-7 and HeLa cells (cytotoxicity assay)

The cytotoxicity of *C. speciosus* (CSEE, CSWF, CSHF, and CSEF) against cancer cells was assessed using the CCK-8/WST-8 reagent, where WST-8 [2-(2-methoxy-4-nitrophenyl)-3-(4-nitrophenyl)-5-(2,4disulfophenyl)-2H-tetrazolium, monosodium salt] was reduced by dehydrogenase in cells to produce an orange-colored formazan, correlated with the number of living cells (20). The IC50 value was calculated using the linear regression equation derived from the data.

CSEE, CSWF, CSHF, and CSEF were dissolved in 1%

DMSO in RPMI-1640. The solution was further prepared in concentrations of 20, 40, 80, 120, and 500 µg/mL in DMSO 1% to calculate the IC50. Furthermore, the cytotoxicity of cisplatin was also evaluated using the same procedure in concentrations of 0.2, 0.4, 1.2, 2.4, and 5.0 µg/mL. Cisplatin was used as the standard drug.

Effect of *Costus speciosus* on the MCF-7 and HeLa cell cycle (flow cytometry apoptotic assay)

This assay is carried out to observe the percentage of MCF-7 and HeLa cells that have undergone apoptosis after the cells are exposed to CSEF (the most cytotoxic fraction) for 24 hours. This assay was performed by following a standard procedure. Apoptosis is detected by initially staining the cells with annexin V-propidium iodide solution followed by flow cytometry analysis. Cells that are not stained with annexin V (AV) or propidium iodide (PI) are viable and will scatter in the Q4 area. Cells that are only stained with AV represent early-stage apoptosis and will scatter in the Q3 area; cells that are stained with both PI and AV show late apoptosis and secondary necrosis and will scatter in the Q2 area; cells that are stained with only PI represent necrosis and will scatter in the Q1 area. Normal cells are hydrophobic as they express phosphatidyl serine within the inner membrane. When the cells undergo apoptosis, the inner membrane flips to become the outer membrane, exposing phosphatidyl serine, which eventually is detected and stained by AV. PI binds and stains the DNA leaks from necrotic cells (21).

Molecular docking simulation

Molecular docking simulation of diosgenin and beta-sitosterol was performed by following a previously described method (22-24) as follows:

Hardware used was MacBook Pro (13-inch, M1, 2020), macOS Ventura, with Chip Apple M1 processor, and a memory of 8 GB. Software used was MarvinSketch 17.11.0 (Academic License), LigandScout 4.1.4 (Universitas Padjadjaran License), AutoDock 4.2 (https://autodock.scripps.edu/), and MacPyMOL: PyMOL 1.7.4.5 Edu.

The macromolecule was the X-ray crystallographic 3D structure of human caspase-3 in complex with tethered salicylate (PDB ID 1NME with a resolution of 1.6 Å; DOI: https://doi.org/10.2210/pdb1NME/pdb) deposited by Erlanson et al. (2003) (25). The protein was downloaded from the Protein Data Bank (https://www.rcsb.org/).

The 2D structure of diosgenin and beta-sitosterol was drawn using the MarvinSketch program and then converted into a 3D structure by applying energy minimization using the Merck molecular force field 94 (MMFF94) method in the LigandScout program. The grid box position and size of the active site were determined automatically by the LigandScout program based on the position of the native ligand as a reference. Molecular docking simulation was done using AutoDock 4.2 embedded in the LigandScout program.

Results

Extraction and fractionation

The yield of the ethanol extract of *C. speciosus* (CSEE) obtained from approximately 770 g of the dried leaves was 4.9 g. The further fractionation of CSEE yielded 21.15 g of water fraction (CSWF), 5.02 g of n-hexane fraction (CSHF), and 2.49 g of ethyl acetate fraction (CSEF).

Effect of *Costus speciosus* on the % survival rate of MCF-7 cells (cytotoxicity assay)

Costus specious indicated a potential to inhibit the % survival rate of MCF-7 cells (depicted in Figure 1) as revealed by the IC50 value of CSEE = 382.32 µg/mL, CSWF = 362.62 µg/mL, CSHF = 185.42 µg/mL, CSEF = 58.71 µg/mL (calculated from the regression equation). The best cytotoxic activity is shown by CSEF. The IC50 value of cisplatin was 3.76 µg/mL confirming a strong cytotoxicity towards MCF-7 cells.

Effect of *Costus speciosus* on the % survival rate of HeLa cells (cytotoxicity assay)

Costus specious indicated weak potential to inhibit the % survival rate of HeLa cells (depicted in Figure 2) as indicated by the IC_{50} value of CSEE = 350.70 µg/mL, CSWF = 764.26 µg/mL, CSHF = 376.57 µg/mL, CSEF = 233.881 µg/mL. The IC_{50} value of cisplatin was 3.78 µg/mL indicating strong cytotoxicity towards HeLa cells.

Effect of the ethyl acetate fraction of *Costus speciosus* (CSEF) on the MCF-7 cell cycle (flow cytometry apoptotic assay)

The effect of CSEF on the MCF-7 cell cycle is presented in Figure 3. Exposure of CSEF (29.35 µg/mL) to MCF-7 cells for 24 hours resulted in 68.85% viability, 22.9% early-stage apoptosis, 5.375% late apoptosis and secondary necrosis, and 2.895% necrosis (Figure 3b), while a very low concentration of cisplatin exposure (1.88 µg/mL) resulted in 3.07% early-stage apoptosis, 3.17% late-stage apoptosis and secondary necrosis, and 0.135% necrosis (Figure 3c).

Effect of the ethyl acetate fraction of *Costus speciosus* (CSEF) on the HeLa cell cycle (flow cytometry apoptotic assay)

The effect of CSEF on the HeLa cell cycle is presented in Figure 4. Exposure of CSEF (29.35 µg/mL) to HeLa cells for 24 hours resulted in an average of 39.45% viability, 3.07% early-stage apoptosis, 16.66% late-stage apoptosis and secondary necrosis, and 40.85% necrosis (Figure 4b), while a very low concentration of cisplatin exposure (1.88 µg/mL) resulted in 10.03% early-stage apoptosis, 9.83% late apoptosis and secondary necrosis, and 2.65% necrosis (Figure 4c).

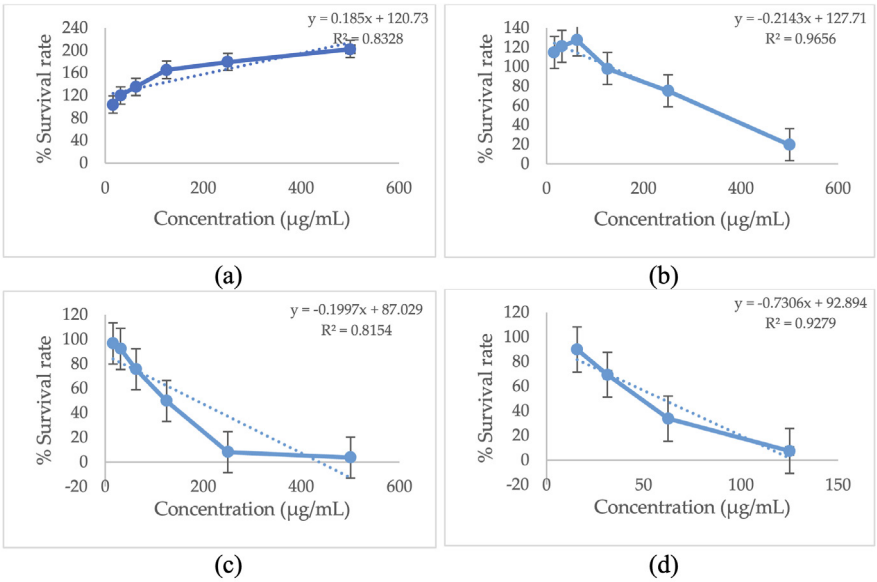

Figure 1. The effect of *Costus speciosus* on the % survival rate of MCF-7 cells. (a) ethanol extract (CSEE) with the regression equation of $y = 0.185x + 120.73$ and correlation coefficient $R^2 = 0.8328$; (b) water fraction (CSWF) with the regression equation of $y = -0.2143x + 127.71$ and correlation coefficient $R^2 = 0.9656$; (c) n-hexane fraction (CSHF) with the regression equation of $y = -0.1997x + 87.029$ and correlation coefficient $R^2 = 0.8154$; (d) ethylacetate fraction (CSEF) with the regression equation of $y = -0.7306x + 92.894$ and correlation coefficient of $R^2 = 0.9279$.

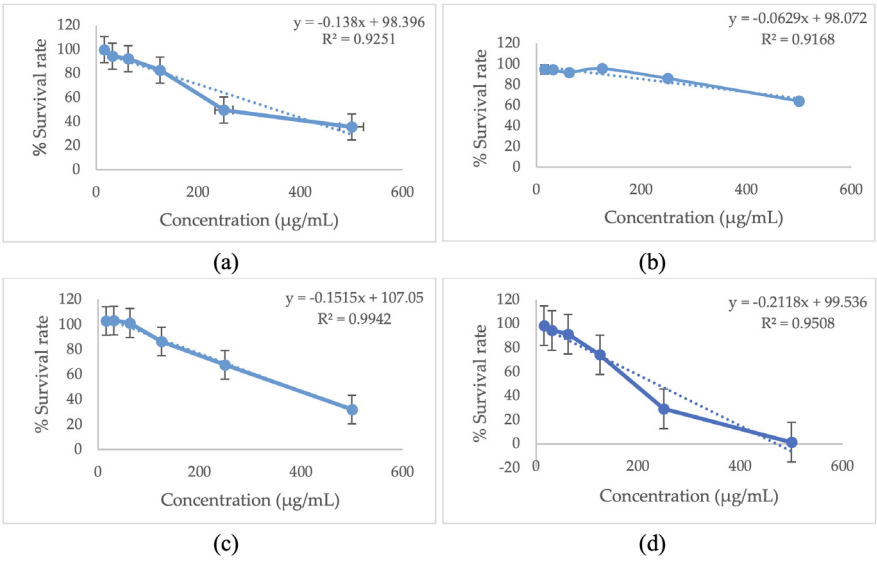

Figure 2. The effect of *Costus speciosus* on the % survival rate of HeLa cells. (a) ethanol extract (CSEE) with the regression equation of $y = -0.138x + 98.396$ and correlation coefficient $R^2 = 0.9251$; (b) water fraction (CSWF) with the regression equation of $y = -0.0629x + 98.072$ and correlation coefficient of $R^2 = 0.9168$; (c) n-hexane fraction (CSHF) with the regression equation of $y = -0.1515x + 107.05$ and correlation coefficient of $R^2 = 0.9942$; (d) ethylacetate fraction (CSEF) with the regression equation of $y = -0.2118x + 99.536$ and correlation coefficient of $R^2 = 0.9508$.

Molecular docking simulation of diosgenin and beta-sitosterol to the active site of caspase-3

Both diosgenin and beta-sitosterol are hydrophobic molecules as confirmed by their cLogP values of 5.428 and 8.025, respectively. The molecular docking simulation revealed that diosgenin could interact with caspase-3 residues, e.g., one hydrogen bond with Asn208 and three hydrophobic interactions with Trp214, Phe247, and Phe250 (binding affinity -8.31 kcal/mol) (Figure 5a), while beta-sitosterol only builded hydrophobic interactions with Trp206, Trp214, Phe247, and Phe256 (binding affinity -6.90 kcal/mol) (Figure 5b). Cisplatin, however, interacted with Gln217 and Asp211.

Discussion

There are three findings of this study: (1) the ethyl acetate fraction, partitioned from the ethanol extract of *Costus speciosus* leaves (CSEF), inhibits the survival growth rate

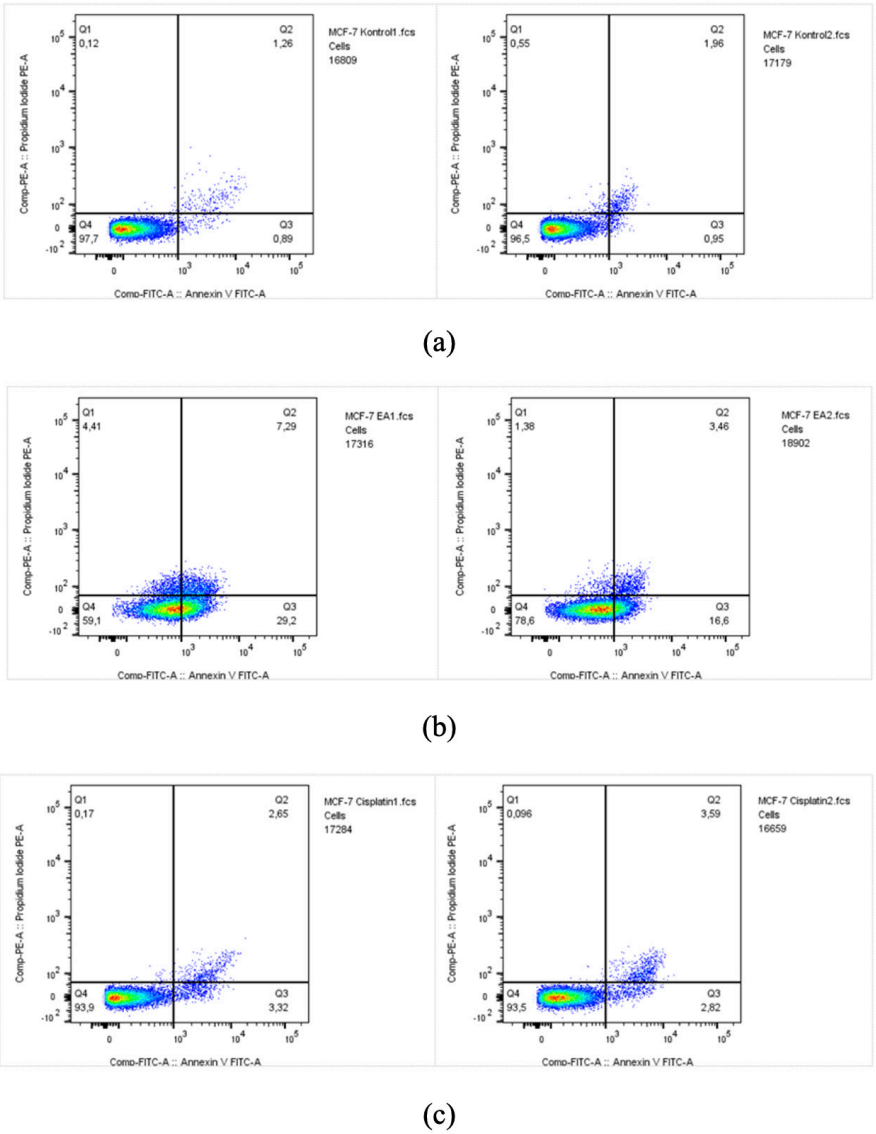

Figure 3. The flow cytometry analysis of MCF-7 cells. (a) MCF-7 cells without treatment; (b) MCF-7 cells exposed to CSEF (29.35 µg/mL); (c) MCF-7 cells exposed to cisplatin (1.88 µg/mL). The analysis was done with two replications. The cells stained with annexin V (AV) or propidium iodide (PI) are living cells and are scattered in the Q4 area. The cells only stained with AV represent early-stage apoptosis and are scattered in the Q3 area; The cells stained with both PI and AV show late apoptosis and secondary necrosis and are scattered in the Q2 area; The cells stained with only PI represent necrosis and are scattered in the Q1 area. Q1 = PI (+), AV (-); Q2 = PI (+), AV (+); Q3 = PI (-), AV (+); Q4 = PI (-), AV (-).

of MCF-7 cells mainly at the early-stage apoptosis of the cell cycle, (2) the ethyl acetate fraction, partitioned from the ethanol extract of *Costus speciosus* (CSEF), inhibits the survival growth rate of HeLa cells by necrosis mechanism, and (3) diosgenin and beta-sitosterol could interact with Trp206, Trp214, Phe247, and Phe250 in the catalytic site of caspase-3.

In our study, CSEF inhibited the survival growth rate of MCF-7 and HeLa cells by apoptosis and necrosis mechanisms. Similarly, previous studies reported that the methanol extracts of *C. speciosus* could inhibit the growth of liver cancer cells (HepG2) (11,12), triple-negative breast cancer (MDA-MB-231) cells (8), and human colon adenocarcinoma (COLO 320DM) cells (13).

Numerous secondary metabolites have been reported to contain in *C. speciosus,* which include, diosgenin, tigogenin, beta-sitosterol, 5α-stigmast-9 (11)-en-3β-ol, β-sitosterol-β-D-glucoside, dioscin, prosapogenins A and B of dioscin, gracillin, α-tocopherol, diosgenone, cycloartanol, 25-en-cycloartenol, and octacosanoic acid (26,27). Our molecular docking simulation explored the binding mode and affinity of diosgenin and beta-sitosterol toward amino acid residues in the catalytic site of cysteine-aspartyl protease-3 (caspase-3). Diosgenin is a plant steroid, described to be a potential bioactive molecule with numerous important medicinal properties, including antihyperlipidemic, antihyperglycemic, antioxidant, anti-inflammatory, and antiproliferative activities. Its

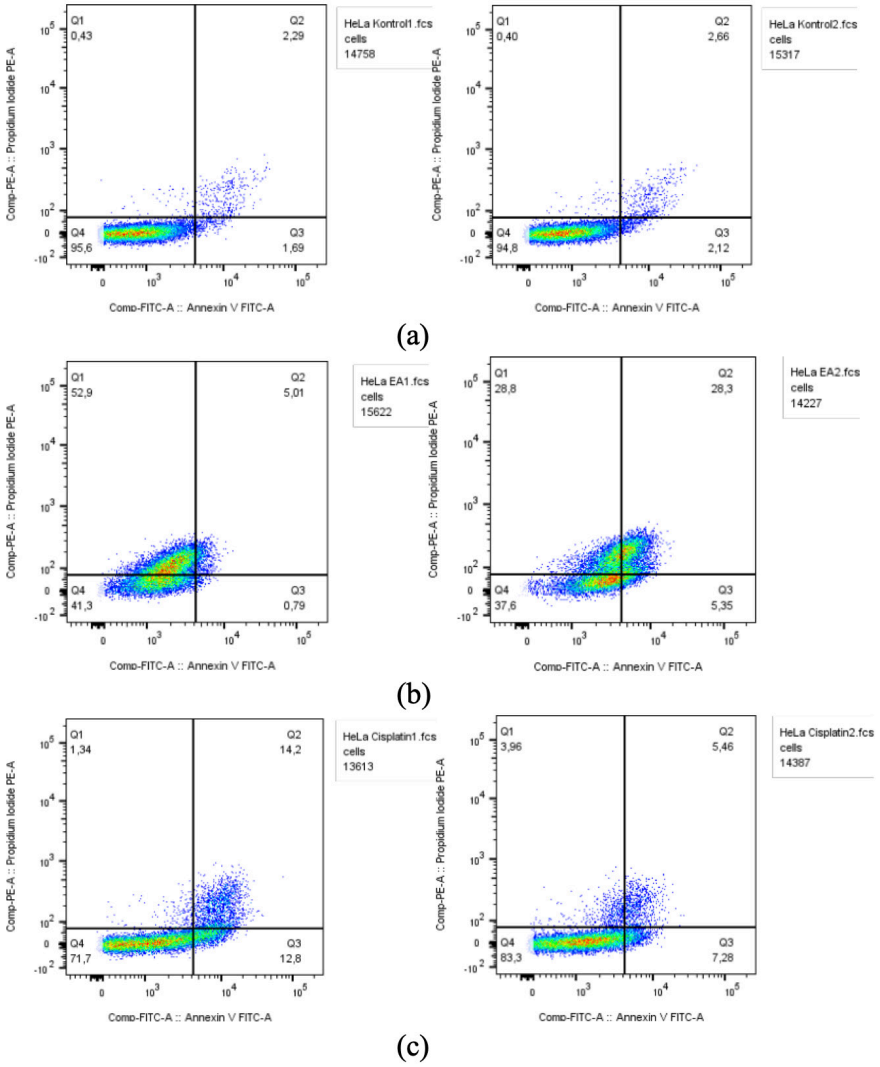

Figure 4. The flow cytometry analysis of HeLa cells. (a) HeLa cells without treatment; (b) HeLa cells exposed to CSEF (29.35 µg/mL); (c) HeLa cells exposed to cisplatin (1.88 µg/mL). The analysis was done with two replications. The cells not stained with annexin V (AV) or propidium iodide (PI) are living cells and are scattered in the Q4 area. The cells only stained with AV represent early-stage apoptosis and are scattered in the Q3 area; the cells stained with both PI and AV show late apoptosis and secondary necrosis and are scattered in the Q2 area; The cells stained with only PI represent necrosis and are scattered in the Q1 area. Q1 = PI (+), AV (-); Q2 = PI (+), AV (+); Q3 = PI (-), AV (+); Q4 = PI (-), AV (-).

anticancer activity is exhibited via several mechanisms. This phytosterol is found in many plants. It was reported to alter cell cycle distribution and stimulate apoptosis in the human osteosarcoma cell line. Cells exposed to diosgenin show an activation of p53 and cell cycle arrest (28). Moreover, diosgenin could induce G2/M cell cycle arrest and apoptosis in human hepatocellular carcinoma (HepG2 HCC) cells (29). Diosgenin induces apoptosis, cell cycle arrest, and COX activity in osteosarcoma (1547) cells (30). The apoptotic activity of diosgenin was described via the upregulation of caspase-3 (31-38), upregulation of caspase-8 (29,32), and upregulation of caspase-9 (29,31,33). Diosgenin also shows activity to down-regulate Bcl-2 and Bcl-xl (31,39,40). Beta-sitosterol is abundantly contained in vegetables, nuts, seeds, grains, and olive oil. This phytosterol was described to impede the viability of MCF-7 and MDA-MB-231 by altering the PI3K/Akt/mTOR pathway (41). Beta-sitosterol damages the morphology of human cervical cancer cells (CaSki and HeLa) by increasing electron density in the cell membrane and decreasing organelles (42). Beta-sitosterol does not modulate the expression of Bcl-xL and Bax in U937 cells; however, it can downregulate Bcl-2, thus suggesting a correlation between caspase-3 activation with Bcl-2 downregulation (43).

Cysteine-aspartyl proteases (caspases) are a unique family of cysteine proteases that execute apoptosis. Caspases exist as inactive zymogens in cells, held together as a dimer with a hydrophobic interface between the monomers, and undergo a cascade of catalytic activation at the onset of apoptosis. These enzymes can be inhibited by the inhibitor of apoptosis family of proteins (44). Caspases involved in apoptosis are categorized into (1) the initiator caspases (e.g., caspase-8 and caspase-9) and

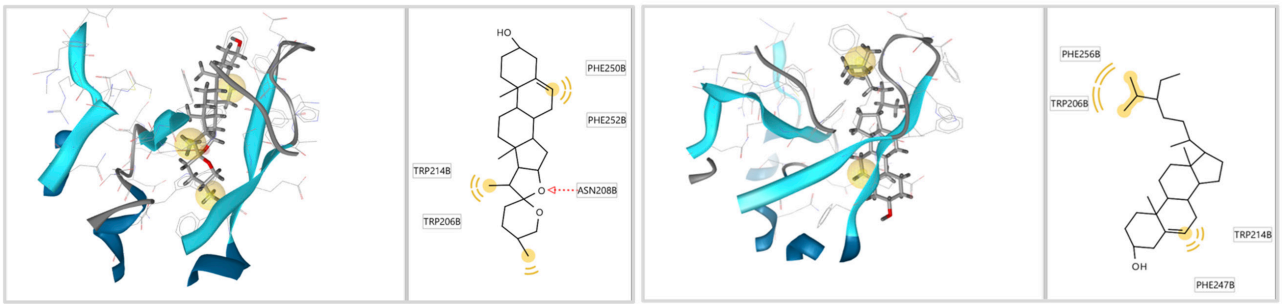

Figure 5. Molecular docking simulation of (a) diosgenin and (b) beta-sitosterol to the active site of caspase-3. Hydrogen bond is shown by a dashed arrow; hydrophobic interaction is shown by a yellow highlight or yellow sphere; the beta-sheet of the protein is shown in blue color. Diosgenin (cLogP of 5.428) builds a hydrogen bond with Asn208 and three hydrophobic interactions with Trp214, Phe247, and Phe250, while beta-sitosterol (cLogP of 8.025) builds four hydrophobic interactions with Trp206, Trp214, Phe247, and Phe256.

(2) the effector caspases (e.g., caspases-3 and -7) (45). Proapoptotic stimuli activate the initiator caspases, which eventually activate the effector caspases by proteolytic intrachain cleavage that changes the conformational of the active site of the effector caspases at amino acid residue Cys163 (46). The S1' pocket of caspase-3 is encircled by four loops building an internal space of 900 $Å^3$. Thr166 and Tyr204 are located on one side of this pocket and Phe128 and Met61 are on the other side, thus allowing a bulky hydrophobic molecule to enter deeply into this groove (47). A previous study described that Ac-DEVD-AFC, a caspase-3 substrate, builts hydrogen bonds with Arg64, Gln161, Arg207, Ser205, Ser209, and hydrophobic interactions to Phe256, Trp206, Trp214 (48). Our molecular docking simulation revealed that diosgenin and beta-sitosterol could interact with Trp206, Trp214, Phe247, and Phe250 in the catalytic site of caspase-3 similar to the binding mode of the caspase-3 substrate, with considerable affinity.

In this study, we used cisplatin as the standard anticancer drug. This well-known chemotherapeutic agent alkylates DNA and builds platinum-DNA adducts, leading to damage in the cancer cells, G1/S arrest, alteration of gene regulation, direct cytotoxicity mediated by reactive oxygen species, and apoptosis (4). Cisplatin was reported to activate the initiator caspases-8, -9, and -2, and the executioner caspase-3 after eight hours of exposure to p35-transfected LLC-PK1 porcine kidney cells (49). Cisplatin blocks the spread of cancer cells during the early steps of the epithelial-mesenchymal transition. It antagonizes the signaling pathway of transforming growth factor-beta by reducing the transcription of many genes responsible for cancer metastasis (50,51). However, in long-term use of cisplatin, resistance may develop. Cisplatin could induce cell death in mesothelioma cells, which was characterized by mitochondrial depolarization, phosphatidylserine translocation, and caspase activation (52). It was reported that two geriatric male patients (ages 62 and 64 years old) diagnosed with esophageal cancer developed severe kidney damage after chemotherapy with cisplatin and 5-fluorouracil. The levels of serum creatinine escalated gradually hence, hemodialysis was required (53). It is acknowledged that approximately thirty percent of patients who are subjected to cisplatin chemotherapy will experience nephrotoxicity due to a higher cisplatin accumulation in this organ through mediated transport (54). Conversely, in a study of 56 patients with cisplatin treatment who developed moderate renal dysfunction, none required hemodialysis. This chemotherapy drug was tolerated at doses of 35-80 mg/m^2 in these patients (55). Cisplatin therapy in a 62-year-old diagnosed with head and neck cancer without risk factors for vascular disease could cause a thromboembolic acute mesenteric ischemia of the small bowel. It is concluded that cisplatin may increase the risk of arterial thrombosis (56).

Conclusion

This study mainly focused on the cytotoxic and apoptotic activity of *C. speciosus* (Koenig) Smith leaves and confirmed that exposure of the ethyl acetate fraction, partitioned from the ethanol extract, to the human breast cancer (MCF-7) and human cervical (HeLa) cells could induce cytotoxicity. The cytotoxicity mechanism is either at the early apoptosis stage on MCF-7 cells or by necrosis on HeLa cells as such is enabled through a reduction in the integrity of mitochondrial, thus unlocking the potential of the plant to be further explored for its anticancer activity.

Acknowledgments

The authors thank to (1) the Ministry of Education, Culture, Research, and Technology of the Republic of Indonesia for funding this project via the Fundamental Grant 2023, and (2) the Rector of Padjadjaran University for funding the APC.

Authors' contribution

Conceptualization: Eli Halimah.
Data curation: Gofarana Wilar, Jutti Levita.
Formal analysis: Gofarana Wilar, Ferry Ferdiansyah Sofyan, Sandra Megantara.

Methodology: Eli Halimah, Sandra Megantara, Gofarana Wilar, Jutti Levita.
Supervision: Eli Halimah.
Validation: Eli Halimah, Jutti Levita.
Writing-original draft: Eli Halimah, Gofarana Wilar.
Writing-review and editing: Jutti Levita, Sandra Megantara.

Availability of data and materials

The datasets used and/or analyzed during the present study are available from the first author upon reasonable request.

Conflict of interests

There is nothing to declare.

Ethical considerations

This study did not use animals, does not apply to humans, and is not mandatory for ethical approval and consent to participate.

Funding/Support

This research was funded by the Ministry of Education, Culture, Research, and Technology of the Republic of Indonesia via the Fundamental Grant 2023 (number 148/E5/PG.02.00.PL/2023 and 3018/UN6.3.1/PT.00/2023), and the APC was funded by Padjadjaran University via the Directorate of Research and Community Engagement.

References

1. World Health Organization (WHO). Global Cancer Burden Growing, Amidst Mounting Need for Services. Available from: https://www.who.int/news/item/01-02-2024-global-cancer-burden-growing--amidst-mounting-need-for-services. Accessed March 27, 2024.
2. Alizadeh AM, Shiri S, Farsinejad S. Metastasis review: from bench to bedside. Tumour Biol. 2014;35(9):8483-523. doi: 10.1007/s13277-014-2421-z.
3. Dizdaroglu M, Jaruga P, Birincioglu M, Rodriguez H. Free radical-induced damage to DNA: mechanisms and measurement. Free Radic Biol Med. 2002;32(11):1102-15. doi: 10.1016/s0891-5849(02)00826-2.
4. Wang H, Guo S, Kim SJ, Shao F, Ho JWK, Wong KU, et al. Cisplatin prevents breast cancer metastasis through blocking early EMT and retards cancer growth together with paclitaxel. Theranostics. 2021;11(5):2442-59. doi: 10.7150/thno.46460.
5. Khoobi M, Foroumadi A, Emami S, Safavi M, Dehghan G, Heidary Alizadeh B, et al. Coumarin-based bioactive compounds: facile synthesis and biological evaluation of coumarin-fused 1,4-thiazepines. Chem Biol Drug Des. 2011;78(4):580-6. doi: 10.1111/j.1747-0285.2011.01175.x.
6. Azizmohammadi M, Khoobi M, Ramazani A, Emami S, Zarrin A, Firuzi O, et al. 2H-chromene derivatives bearing thiazolidine-2,4-dione, rhodanine or hydantoin moieties as potential anticancer agents. Eur J Med Chem. 2013;59:15-22. doi: 10.1016/j.ejmech.2012.10.044.
7. Ramazani A, Khoobi M, Torkaman A, Zeinali Nasrabadi F, Forootanfar H, Shakibaie M, et al. One-pot, four-component synthesis of novel cytotoxic agents 1-(5-aryl-1,3,4-oxadiazol-2-yl)-1-(1H-pyrrol-2-yl)methanamines. Eur J Med Chem. 2014;78:151-6. doi: 10.1016/j.ejmech.2014.03.049.
8. Gheraibia S, Belattar N, Abdel-Wahhab MA. HPLC analysis, antioxidant and cytotoxic activity of different extracts of *Costus speciosus* against HePG-2 cell lines. S Afr J Bot. 2020;131:222-8. doi: 10.1016/j.sajb.2020.02.019.
9. da Silva BP, Bernardo RR, Parente JP. Flavonol glycosides from *Costus spicatus*. Phytochemistry. 2000;53(1):87-92. doi: 10.1016/s0031-9422(99)00441-0.
10. Binny K, Kumar SG, Dennis T. Anti-inflammatory and antipyretic properties of the rhizome of *Costus speciosus* (koen.) Sm. J Basic Clin Pharm. 2010;1(3):177-81.
11. Bawakid NO, Abdel-Lateff A, El-Senduny FF, Alarif WM. *Costus speciosus* J Koenig (Costaceae) exerts anti-proliferative effect on breast cancer cells via induction of cell cycle arrest and inhibition of activity of metalloproteinase-2. Trop J Pharm Res. 2021;20(7):1365-72. doi: 10.4314/tjpr.v20i7.7.
12. Nair SV, Hettihewa M, Rupasinghe HP. Apoptotic and inhibitory effects on cell proliferation of hepatocellular carcinoma HepG2 cells by methanol leaf extract of *Costus speciosus*. Biomed Res Int. 2014;2014:637098. doi: 10.1155/2014/637098.
13. Baskar AA, Al Numair KS, Alsaif MA, Ignacimuthu S. In vitro antioxidant and antiproliferative potential of medicinal plants used in traditional Indian medicine to treat cancer. Redox Rep. 2012;17(4):145-56. doi: 10.1179/1351000212y.0000000017.
14. de Siqueira EP, Ramos JP, Zani CL, de Oliveira Nogueira AC, Nelson DL, de Souza-Fagundes EM, et al. *Chamaecostus subsessilis* and *Chamaecostus cuspidatus* (Nees & Mart) C.Specht and D.W.Stev as potential sources of anticancer agents. Nat Prod Chem Res. 2016;4:204. doi: 10.4172/2329-6836.1000204.
15. Naznin NE, Mazumder T, Reza MS, Jafrin S, Alshahrani SM, Alqahtani AM, et al. Molecular docking supported investigation of antioxidant, analgesic and diuretic effects of *Costus speciosus* rhizome. Bull Chem Soc Ethiop. 2022;36(3):627-40. doi: 10.4314/bcse.v36i3.12.
16. Pawar VA, Pawar PR. *Costus speciosus*: an important medicinal plant. Int J Sci Res. 2014;3(7):28-33.
17. Dai J, Mumper RJ. Plant phenolics: extraction, analysis and their antioxidant and anticancer properties. Molecules. 2010;15(10):7313-52. doi: 10.3390/molecules15107313.
18. Scarano P, Tartaglia M, Zuzolo D, Prigioniero A, Guarino C, Sciarrillo R. Recovery and valorization of bioactive and functional compounds from the discarded of *Opuntia ficus-indica* (L.) Mill. fruit peel. Agronomy. 2022;12(2):388. doi: 10.3390/agronomy12020388.
19. Mutakin, Saptarini NM, Amalia R, Sumiwi SA, Megantara S, Saputri FA, et al. Molecular docking simulation of phenolics towards tyrosinase, phenolic content, and radical scavenging activity of some Zingiberaceae plant extracts. Cosmetics. 2023;10(6):149. doi: 10.3390/cosmetics10060149.
20. Cai L, Qin X, Xu Z, Song Y, Jiang H, Wu Y, et al. Comparison of cytotoxicity evaluation of anticancer drugs between real-time cell analysis and CCK-8 method. ACS Omega. 2019;4(7):12036-42. doi: 10.1021/acsomega.9b01142.
21. Lakshmanan I, Batra SK. Protocol for apoptosis assay by flow cytometry using annexin V staining method. Bio Protoc. 2013;3(6):e374. doi: 10.21769/bioprotoc.374.
22. Megantara S, Wathoni N, Mohammed AF, Suhandi C, Ishmatullah MH, Putri M. In silico study: combination of

α-mangostin and chitosan conjugated with trastuzumab against human epidermal growth factor receptor 2. Polymers (Basel). 2022;14(13):2447. doi: 10.3390/polym14132747.
23. Lesmana R, Ade FY, Pratiwi YS, Goeanawan H, Sylviana N, Megantara S, et al. Potential molecular interaction of nutmeg's (*Myristica fragrans*) active compound via activation of caspase-3. Indones J Sci Technol. 2022;7(1):159-70. doi: 10.xxxxx/ijost.v2i2.
24. Febrina EL, Alamhari RK, Asnawi AI, Abdulah RI, Lestari KE, Levita JU, et al. Molecular docking and molecular dynamics studies of *Acalypha indica* L. phytochemical constituents with caspase-3. Int J Appl Pharm. 2021;13(4):210-5.
25. Erlanson DA, Lam JW, Wiesmann C, Luong TN, Simmons RL, DeLano WL, et al. In situ assembly of enzyme inhibitors using extended tethering. Nat Biotechnol. 2003;21(3):308-14. doi: 10.1038/nbt786.
26. Thambi M, Cherian T. Phytochemical investigation, molecular docking studies, and biological efficacy of rhizome essential oil composition of *Costus speciosus*. In: Arunachalam K, Yang X, Puthanpura Sasidharan S, eds. Natural Product Experiments in Drug Discovery. Springer Protocols Handbooks. New York, NY: Humana; 2023. p. 505-20. doi: 10.1007/978-1-0716-2683-2_30.
27. Qiao CF, Li QW, Dong H, Xu LS, Wang ZT. [Studies on chemical constituents of two plants from *Costus*]. Zhongguo Zhong Yao Za Zhi. 2002;27(2):123-5. [Chinese].
28. Corbiere C, Liagre B, Terro F, Beneytout JL. Induction of antiproliferative effect by diosgenin through activation of p53, release of apoptosis-inducing factor (AIF) and modulation of caspase-3 activity in different human cancer cells. Cell Res. 2004;14(3):188-96. doi: 10.1038/sj.cr.7290219.
29. Li Y, Wang X, Cheng S, Du J, Deng Z, Zhang Y, et al. Diosgenin induces G2/M cell cycle arrest and apoptosis in human hepatocellular carcinoma cells. Oncol Rep. 2015;33(2):693-8. doi: 10.3892/or.2014.3629.
30. Moalic S, Liagre B, Corbière C, Bianchi A, Dauça M, Bordji K, et al. A plant steroid, diosgenin, induces apoptosis, cell cycle arrest and COX activity in osteosarcoma cells. FEBS Lett. 2001;506(3):225-30. doi: 10.1016/s0014-5793(01)02924-6.
31. Liu MJ, Wang Z, Ju Y, Zhou JB, Wang Y, Wong RN. The mitotic-arresting and apoptosis-inducing effects of diosgenyl saponins on human leukemia cell lines. Biol Pharm Bull. 2004;27(7):1059-65. doi: 10.1248/bpb.27.1059.
32. Corbiere C, Liagre B, Terro F, Beneytout JL. Induction of antiproliferative effect by diosgenin through activation of p53, release of apoptosis-inducing factor (AIF) and modulation of caspase-3 activity in different human cancer cells. Cell Res. 2004;14(3):188-96. doi: 10.1038/sj.cr.7290219.
33. Cailleteau C, Liagre B, Beneytout JL. A proteomic approach to the identification of molecular targets in subsequent apoptosis of HEL cells after diosgenin-induced megakaryocytic differentiation. J Cell Biochem. 2009;107(4):785-96. doi: 10.1002/jcb.22176.
34. Selim S, Al Jaouni S. Anticancer and apoptotic effects on cell proliferation of diosgenin isolated from *Costus speciosus* (Koen.) Sm. BMC Complement Altern Med. 2015;15:301. doi: 10.1186/s12906-015-0836-8.
35. Das S, Dey KK, Dey G, Pal I, Majumder A, MaitiChoudhury S, et al. Antineoplastic and apoptotic potential of traditional medicines thymoquinone and diosgenin in squamous cell carcinoma. PLoS One. 2012;7(10):e46641. doi: 10.1371/journal.pone.0046641.
36. Leger DY, Liagre B, Beneytout JL. Role of MAPKs and NF-kappaB in diosgenin-induced megakaryocytic differentiation and subsequent apoptosis in HEL cells. Int J Oncol. 2006;28(1):201-7.
37. Liu MJ, Wang Z, Ju Y, Wong RN, Wu QY. Diosgenin induces cell cycle arrest and apoptosis in human leukemia K562 cells with the disruption of Ca2+ homeostasis. Cancer Chemother Pharmacol. 2005;55(1):79-90. doi: 10.1007/s00280-004-0849-3.
38. Raju J, Patlolla JM, Swamy MV, Rao CV. Diosgenin, a steroid saponin of *Trigonella foenum graecum* (Fenugreek), inhibits azoxymethane-induced aberrant crypt foci formation in F344 rats and induces apoptosis in HT-29 human colon cancer cells. Cancer Epidemiol Biomarkers Prev. 2004;13(8):1392-8.
39. Srinivasan S, Koduru S, Kumar R, Venguswamy G, Kyprianou N, Damodaran C. Diosgenin targets Akt-mediated prosurvival signaling in human breast cancer cells. Int J Cancer. 2009;125(4):961-7. doi: 10.1002/ijc.24419.
40. Léger DY, Liagre B, Cardot PJ, Beneytout JL, Battu S. Diosgenin dose-dependent apoptosis and differentiation induction in human erythroleukemia cell line and sedimentation field-flow fractionation monitoring. Anal Biochem. 2004;335(2):267-78. doi: 10.1016/j.ab.2004.09.008.
41. Zhu Y, Yao Y, Shi Z, Everaert N, Ren G. Synergistic effect of bioactive anticarcinogens from soybean on anti-proliferative activity in MDA-MB-231 and MCF-7 human breast cancer cells in vitro. Molecules. 2018;23(7):1557. doi: 10.3390/molecules23071557.
42. Baeka J, Rohb HS, Choi CI, Baekb KH, Kim KH. *Raphanus sativus* sprout causes selective cytotoxic effect on p53-deficient human lung cancer cells in vitro. Nat Prod Commun. 2017;12(2):237-40. doi: 10.1177/1934578x1701200224.
43. Sharmila R, Sindhu G. Modulation of angiogenesis, proliferative response and apoptosis by β-sitosterol in rat model of renal carcinogenesis. Indian J Clin Biochem. 2017;32(2):142-52. doi: 10.1007/s12291-016-0583-8.
44. Shi Y. Caspase activation, inhibition, and reactivation: a mechanistic view. Protein Sci. 2004;13(8):1979-87. doi: 10.1110/ps.04789804.
45. Adams JM, Cory S. Apoptosomes: engines for caspase activation. Curr Opin Cell Biol. 2002;14(6):715-20. doi: 10.1016/s0955-0674(02)00381-2.
46. Riedl SJ, Fuentes-Prior P, Renatus M, Kairies N, Krapp S, Huber R, et al. Structural basis for the activation of human procaspase-7. Proc Natl Acad Sci U S A. 2001;98(26):14790-5. doi: 10.1073/pnas.221580098.
47. Fang B. Structural Basis of Caspase-3 Substrate Specificity Revealed by Crystallography, Enzyme Kinetics, and Computational Modeling [dissertation]. Georgia State University; 2009.
48. Megantara S, Mutakin M, Halimah E, Febrina E, Levita J. Molecular interaction of the downstream executioner cysteine aspartyl proteases (caspase-3 and caspase-7) with

corilagin, quercetin, rutin, kaempferol, gallic acid, and geraniin of *Acalypha wilkesiana* Müll. arg. Rasayan J Chem. 2020;13(3):1321-9. doi: 10.31788/rjc.2020.1335766.
49. Bai J, Li Y, Zhang G. Cell cycle regulation and anticancer drug discovery. Cancer Biol Med. 2017;14(4):348-62. doi: 10.20892/j.issn.2095-3941.2017.0033.
50. Kaushal GP, Kaushal V, Hong X, Shah SV. Role and regulation of activation of caspases in cisplatin-induced injury to renal tubular epithelial cells. Kidney Int. 2001;60(5):1726-36. doi: 10.1046/j.1523-1755.2001.00026.x.
51. Wang H, Guo S, Kim SJ, Shao F, Ho JWK, Wong KU, et al. Cisplatin prevents breast cancer metastasis through blocking early EMT and retards cancer growth together with paclitaxel. Theranostics. 2021;11(5):2442-59. doi: 10.7150/thno.46460.
52. Cregan IL, Dharmarajan AM, Fox SA. Mechanisms of cisplatin-induced cell death in malignant mesothelioma cells: role of inhibitor of apoptosis proteins (IAPs) and caspases. Int J Oncol. 2013;42(2):444-52. doi: 10.3892/ijo.2012.1715.
53. Sasaki T, Motoyama S, Komatsuda A, Shibata H, Sato Y, Yoshino K, et al. Two cases of cisplatin-induced permanent renal failure following neoadjuvant chemotherapy for esophageal cancer. Int J Surg Case Rep. 2016;20:63-7. doi: 10.1016/j.ijscr.2016.01.009.
54. Arany I, Safirstein RL. Cisplatin nephrotoxicity. Semin Nephrol. 2003;23(5):460-4. doi: 10.1016/s0270-9295(03)00089-5.
55. Ogawa T, Niho S, Nagai S, Kojima T, Nishimura Y, Ohe Y, et al. Moderate renal dysfunction may not require a cisplatin dose reduction: a retrospective study of cancer patients with renal impairment. Int J Clin Oncol. 2013;18(6):977-82. doi: 10.1007/s10147-012-0481-x.
56. Khosla S, Kennedy L, Abdulaal Y. Cisplatin induced acute mesenteric ischaemia: a case report and review of the literature. Int J Surg Case Rep. 2017;41:347-51. doi: 10.1016/j.ijscr.2017.11.007